Zeitschrift: IABSE reports of the working commissions = Rapports des commissions de travail AIPC = IVBH Berichte der Arbeitskommissionen

Band: 34 (1981)

Artikel: Nonlinear finite elements analysis of reinforced concrete beam-column joints

Autor: Noguchi, H.

DOI: https://doi.org/10.5169/seals-26921

Nonlinear Finite Elements Analysis of Reinforced Concrete Beam-Column Joints

Analyse non-linéaire par éléments finis de la liaison entre poutre et colonne en béton armé.

Nichtlineare Finite-Elemente-Berechnung von Träger-Stützen-Verbindungen

H. NOGUCHI
Associate Professor
Dep. of Arch. Eng., Fac. of Eng.
Chiba University
Chiba, Japan

SUMMARY
The nonlinear behavior of reinforced concrete beam-column joints is analyzed by the finite element model combining the individual material properties with emphasis on the effect of the different bond characteristics of beam bars through the joint. Comparisons are presented with tests for deflection behavior, crack propagation, strain distributions of beam and column longitudinal bars, strain of ties and bond slips of beam bars through the joint. The effects of the truss mechnism and loss of bond on the strain distribution of beam bars and the shear resistance mechnism of the joint are discussed.

RÉSUMÉ
Le comportement non-linéaire de jonctions colonne-poutre en béton armé est analysé par éléments finis. L'analyse tient compte tant des propriétés individuelles des matériaux que des effets des différentes caractéristiques d'adhésion entre armatures et béton. La comparaison est faite avec des essais mésurant le comportement à la flexion, à la fissuration, à la distribution des déformations des armatures longitudinales de la poutre et de la colonne, à la déformation des étriers et le glissement des armatures principales au niveau de le jonction. L'effet du mécanisme de treillis et de la perte d'adhésion sur la distribution des déformations des armatures et sur le mécanisme de résistance au cisaillement de la jonction est discuté.

ZUSAMMENFASSUNG
Das nichtlineare Verhalten von Träger-Stützen-Verbindungen aus Stahlbeton wurde mit finiten Elementen untersucht, wobei der Nachdruck auf die Verbundeigenschaften gelegt wurde. Versuchsergebnisse wurden in Bezug auf Durchbiegung, Rissbildung, Dehnungsverteilung und Relativverschiebung zwischen Bewehrung und Beton verglichen. Fachwerkwirkung und Verbundversagen werden diskutiert.

1. INTRODUCTION

The stress level recently becomes very severe in the reinforced concrete (RC) beam-column joints subjected to earthquakes for the following backgrounds. The high strength and large-sized deformed bar was developed and the dimension of sections in beams or columns is getting smaller. As the shear strength of beams and columns is getting reinforced according to the revised building code in Japan, the beam-column joint is getting a relatively weak point.

The mechanical characteristics of the RC beam-column joint are mainly composed of the following two elements:

1. The shear resistance mechanism after inclined cracks initiate in the joint.
2. The bond slip mechanism of beam longitudinal bars through the joint.

Especially the bond slip of beam longitudinal bars through the joint for the bond deterioration has great influences on the story deflection and the restoring force characteristics of overall structures.

There are many active experimental studies for the beam-column joints. Recently the effects of lateral beams [1], eccentric beams [2] and biaxial loading [3] are discussed. As for analytical studies, the works of Shimohira [4], Will [5], Mirza [6], Ohtsuki [7], Ohwada [8], Ichinose [9] and Tada [10] are listed, but the nonlinear behavior after the initiation of the inclined crack in the joint has been scarcely discussed.

In this study the modeling of material properties is carried out in accordance with the previous experimental studies and the analytical results obtained by the finite element method are compared with the test results.

2. ANALYTICAL MODELS

2.1 General

The effects of lateral beams, eccentric beams and the confinement of ties are originally three-dimensional problems. In this study the subject of analysis is limited to the joint without the lateral beams or the eccentric beams, and the plane stress state is assumed.

2.2 Concrete

Concrete is represented by the linearly varying strain triangular element with six nodal points which was originally developed by Felippa [11], as shown in Fig.1. In this element the current stress-strain matrices are decided at corner points and midpoints. The element is subdivided into 4 subtriangles. Inside each subtriangle the entries of the stress-strain matrix are assumed to vary linearly.

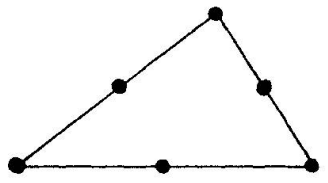

Fig.1 Triangular Element for Concrete and Longitudinal Bar

The analytical model used to represent the behavior of concrete under biaxial stresses in this study was originally developed by Darwin [12], [13], [14]. The author [15], [16] compared a model based on the theory of plasticity and using Drucker-Prager's yield criterion, which had been used by many investigators, and four other models with the test results of Kupfer [17] and Nelissen [18]. He concluded that the plasticity model could not represent the behavior of concrete adequately, especially at higher stress levels, and that the

orthotropic model of Darwin [12 - 14] gave the best results in both principal directions for the models that he considered.

In Darwin's model concrete is assumed to be an orthotropic material in the two principal stress directions. The incremental constitutive relationship referred to the two principal axes are written as follows:

$$\begin{Bmatrix} d\sigma_1 \\ d\sigma_2 \\ d\tau_{12} \end{Bmatrix} = \frac{1}{1-\upsilon^2} \begin{bmatrix} E_1 & \upsilon\sqrt{E_1E_2} & 0 \\ & E_2 & 0 \\ (\text{symm.}) & & \frac{1}{4}(E_1+E_2-2\upsilon\sqrt{E_1E_2}) \end{bmatrix} \begin{Bmatrix} d\varepsilon_1 \\ d\varepsilon_2 \\ d\gamma_{12} \end{Bmatrix} \quad (1)$$

In Eq.(1) both the shear modulus and Poisson's ratio, υ, are assumed to be independent of orientation.

Darwin developed the concept of "equivalent uniaxial strain," ε_{iu}, which is obtained when only the Poisson's effect is removed from the biaxial strains. The total equivalent uniaxial strain at any point is obtained as follows:

$$\varepsilon_{iu} = \Sigma\, d\varepsilon_{iu} = \Sigma \frac{d\varepsilon_i}{(1-\upsilon\alpha n)} = \Sigma \frac{d\sigma_i}{E_i} \quad (2)$$

where $\alpha = \sigma_1/\sigma_2$ = biaxial stress ratio
$n = E_2/E_1$ = modular ratio.

The "equivalent uniaxial" stress-strain curves for compressive loading are based on the following equation suggested by Saenz [19].

$$\sigma_i = \frac{E_0\varepsilon_{iu}}{1+\left(\frac{E_0}{E_s}-2\right)\frac{\varepsilon_{iu}}{\varepsilon_{ic}}+\left(\frac{\varepsilon_{iu}}{\varepsilon_{ic}}\right)^2} \quad (3)$$

where E_0 = initial uniaxial tangent modulus
$E_s = \sigma_{ic}/\varepsilon_{ic}$ = secant modulus
$\sigma_{ic}, \varepsilon_{ic}$ = maximum compressive stress and corresponding equivalent uniaxial strain in principal direction, i.

As the crack pattern is predicted from the test results in this study, the elasticity is assumed for tension.

$$\sigma_i = E_0\varepsilon_{iu} \quad (4)$$

The values of the maximum stresses in the two principal directions, σ_{1c}, σ_{2c}, are obtained from the modified biaxial strength envelope of Kupfer and Gerstle [17] which is shown in Fig.2.

For values of strength greater than f'_c in absolute magnitude, a relatively large strain at the maximum stress, was indicated by Kupfer [20].

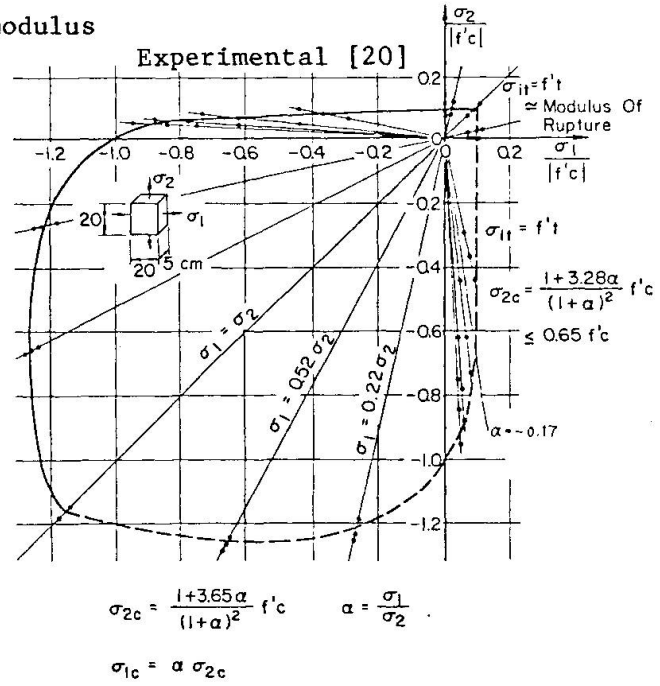

Fig.2 Biaxial Strength Envelope Used in the Present Study

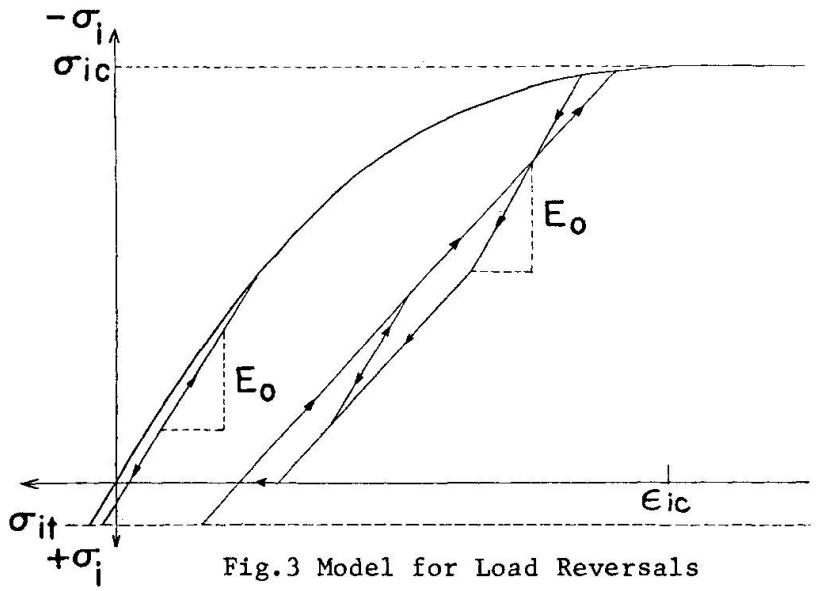

Fig.3 Model for Load Reversals

To include this behavior in the model, the variation of ϵ_{ic} at the maximum compressive stress, σ_{ic}, is determined from the experimental stress-strain curve and it is given in Refs. [12], [14].

The variation of Poisson's ratio is assumed as follows:

$$\upsilon = 0.2 \qquad \text{for tension-tension and compression-compression} \qquad (5)$$

$$\upsilon = 0.2 + 0.6\left(\frac{\sigma_2}{f'_c}\right)^4 + 0.4\left(\frac{\sigma_1}{\sigma_{1t}}\right)^4$$

$$\upsilon \leq 0.99 \qquad \text{for uniaxial compression and tension-compression} \qquad (6)$$

where

f'_c = uniaxial compressive strength

σ_{1t} = uniaxial tensile strength

Also for the unloading and reloading curves, Darwin's model is adopted, as shown in Fig. 3. Beyond the maximum compressive strength the strength is kept constant in this study.

2.3 Longitudinal Bar

The linearly varying strain triangular element is used also for the longitudinal bar to represent the dowel action. The constitutive law under biaxial stresses is based on the theory of plasticity using Von Mises's yield criterion. For this study a simplified bilinear model is used for the equivalent stress-strain curve and the rate of strain hardening is set to $0.01E_s$, where E_s is the Young's modulus.

2.4 Stirrup and Tie

The stirrup and tie are represented by the bar elements. A simplified bilinear model is used for the stress-strain curve and the rate of strain hardening is set to $0.05E_{st}$, where E_{st} is the Young's modulus. When the stirrup or tie is a round bar, its anchorage to longitudinal bars is assumed to be carried out at only the exterior nodal points of the londitudinal bar elements.

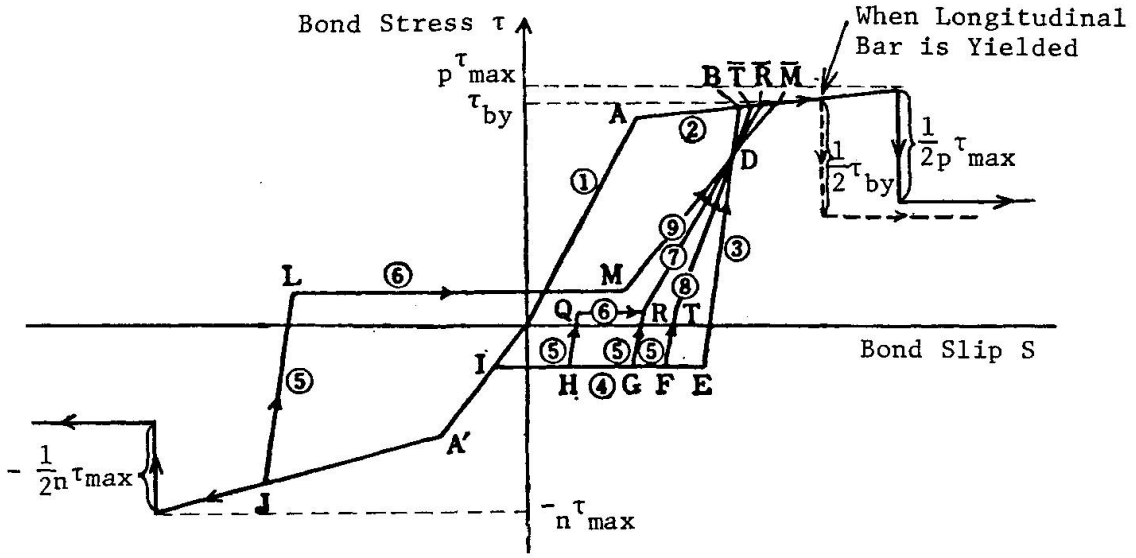

Fig.4 Idealized Bond Stress-Slip Relationships

2.5 Bond Slip

Bond slip is modeled by the bond-link element which was first developed by Ngo and Scordelis [21]. The discussion on the applicability of the bond-link element was made by the author in Refs. [22], [23]. Though there are some problems in the bond-link element, it is rather appropriate to use such a simple model as the bond-link element for the large-scale subject like a beam-column joint.

Slip characteristics parallel to the bar axis are obtained from the modified bond stress-slip relations under cycles of load reversal which were originally proposed by Morita and Kaku [24], [25], as shown in Fig.4. As a modified point for Morita's model, when the bond stress yields the maximum bond strength or the longitudinal bar is yielded, half of the bond stress is released and the bond stiffness is set to zero, as shown in Fig. 4. [26]

For the spring stiffness of the bond-link element perpendicular to the bar axis, about the same relations as those of spring stiffness parallel to the bar axis are used as the first step to represent the sinking or separating of the longitudinal bar which is subjected to the dowel forces.

2.6 Concrete Cracking

The author discussed the modeling of crack initiation and propagation in Refs. [16], [27]. In this study, as the crack pattern is predicted from the previous test results, the crack-link element, as shown in Fig. 5, is put in between two nodes on both faces of the crack. When the principal stress of a node on the predicted cracking surface exceeds the modulus of rupture, a crack occurs along the particular grid line. The crack initiation is represented by setting the spring stiffness both vertical and parallel to the crack surface from the initial large values to zero, and cracking release

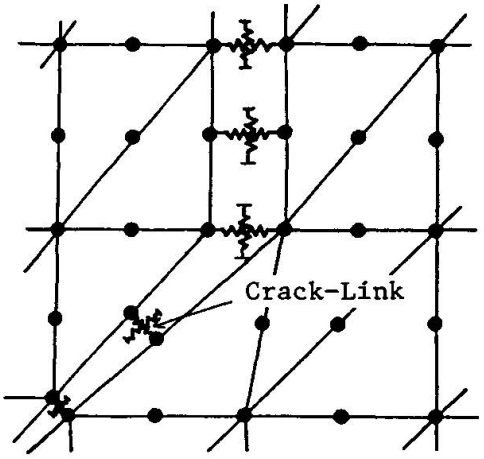

Fig.5 Crack-Link Elements

nodal forces are applied to two nodes on the crack surface at the next iterative step. Therefore, the aggregate interlock on the crack surface is not considered.

The closing or reopening of a crack is judged on the crack width. When a crack is closed, the only vertical spring stiffness to the crack surface is set to the initial large value.

3. NONLINEAR ANALYTICAL METHOD

The load incremental method using the tangent modulus is adopted for the nonlinear analysis [28], [29], [30]. At each loading stage, crack initiation and propagation are checked. The number of the iteration steps at which only cracking release nodal forces are applied is limited to one, and the next crack propagation is treated at the next loading stage.

The frontal method is used for the solution of the simultaneous, linear algebraic equations [28], [29].

4. SPECIMENS FOR SUBJECTS OF ANALYSIS

The beam-column joint specimens tested by Kamimura and Hamada [31] are selected for the subjects of analysis, because there were three specimens with different bond characteristics on beam bars within a joint and the detailed measurements on deformations, strains and bond slips were carried out in their tests. The detailed reinforcement of Kamimura's specimens is shown in Fig. 6. In this study the test results of two specimens, No.1 and No.3 are compared to the analytical results. The specimen No.1 had normal bond and specimen No.3 had almost no bond on beam bars within a joint by applying paraffin on the surface of the beam bar with a thickness of 1 - 2 mm above the rib of the bar.

The finite element idealization of Kamimura's specimen is shown in Fig. 7. Only half of the whole specimen is analyzed due to symmetry around a point. The crack pattern was set up using crack-link elements in general accord with the test results. Steel nodal points on both edges of a longitudinal bar were connected with the corresponding concrete nodal points by bond-link elements. Two bond-link elements were introduced on both faces of a crack. Ties and stirrups were

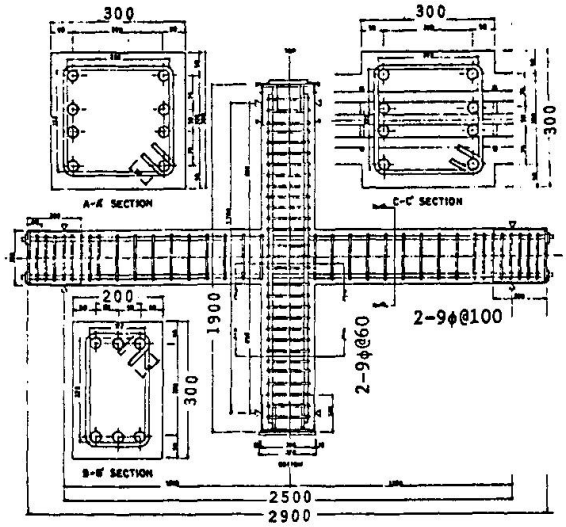

Fig.6 Specimens Tested by Kamimura et al. [31]

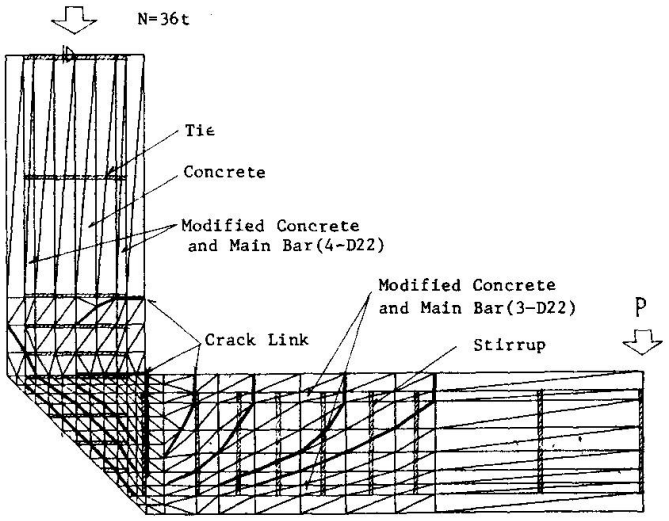

Fig.7 Finite Element Idealization

set up in well accord with those of the test specimen. As they were round bars, their anchorage to longitudinal bars was assumed to be carried out at the exterior nodal points of the longitudinal bar elements.

Test results of local bond stress-slip relations of beam longitudinal bars within a joint are shown for specimen No.1 in Fig. 8. From Fig. 8 it can be stated that the initial bond stiffness and the bond yielding stress are higher in the compression zone of the joint than in the tension zone. These phenomena were shown in tests by other researchers; Tada et al. [32]. In this study, for specimen No.1, bond characteristics of beam longitudinal bars within a joint are given separately in the compression and tension zones, as shown in Fig. 8. Bond characteristics of column longitudinal bars within a joint are given in accordance with those of the beam bars within the joint. Bond characteristics of longitudinal bars in the beam and column are given with reference to the test results of strain distributions, as shown in Fig. 8.

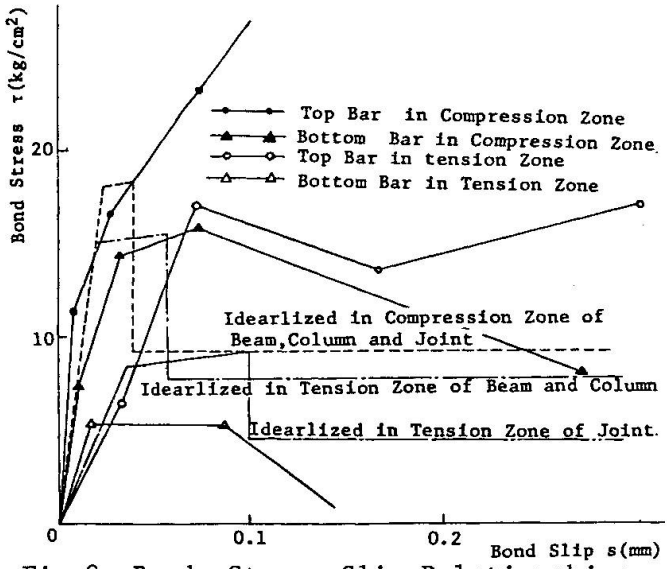

Fig.8 Bond Stress-Slip Relationships

In this study four specimens including specimen No.1 were analyzed as shown in Table 1. They had different bond characteristics on beam bars within a joint.

For specimen No.2 with almost perfect bond , the effect of the truss mechanism after the propagation of the inclined crack in a joint on the strain distribution of beam bars is studied.

For specimen No.3 with almost no bond, the effect of the loss of bond and the truss mechanism on the strain distribution of beam bars and the shear resistance mechanism of the joint is studied from the comparison of the analytical results with the test results.

Table 1. Material Properties Used for the Analysis

Specimen	No.1	No.2	No.3	No.4
Bond Characteristics	Normal Bond	Perfect Bond Truss Mechanism	No Bond	No Bond No Inclined Crack in Joint
Initial Bond Stiffness in Joint (kgf/cm^3)	Tension: 2640 Compression: 8100	2×10^8	20	20
Concrete	$E_0 = 2.54 \times 10^5$kgf/cm^2, $f'_c = -197$kgf/cm^2, $\varepsilon_{cu} = -0.23\%$, $f'_t = 29.6$kgf/cm^2, $_c\upsilon_0 = 0.2$			
Longitudinal Bar SD 35, D22	$E_s = 1.94 \times 10^6$kgf/cm^2, $_y\sigma_s = 3633$kgf/cm^2, $_s\upsilon_0 = 0.3$			
Stirrup and Tie SR 24, 9ϕ	$E_{st} = 1.98 \times 10^6$kgf/cm^2, $_y\sigma_{st} = 3300$kgf/cm^2			

For specimen No.4, in which the initiation of the inclined crack was prohibited and almost no bond was assumed for beams within the joint, only the effect of the loss of bond on the strain distribution of beam bars and shear resistance mechanism is studied.

The variables used to define material models are given in Table 1.

5. PROGRESS OF FAILURE

The analytical results on the condition of deformation and crack propagation for specimen No.1 are shown in Figs. 9 and 10. The comparisons of various analytical cracking and yielding loads with the test results are shown in Table 2.

In the analyses the flexural cracks initiated near the beam joint at the loading stage, P = 1t. These are corresponding to the test results. Then they propagated in the center of the beam span as the load increased. The flexural cracks of the column initiated at the column joint at P = 4t and the cracking load is a little higher than the test results.

The conditions of deformation of the joint and its vicinities at P = 5t are shown in Fig. 11 for No.1, No.2, No.3. From Fig. 11 it can be stated that the effects of bond characteristics are appeared in the flexural crack width at the beam joint. For No.3 the flexural crack at the beam joint propagated very quickly and the crack width amounted to about 1.0mm. For No.1 and No.2 the propagation of the flexural crack was rather slow and the crack width was only 0.15mm for No.2. Meanwhile the propagation of the flexural crack at the column joint was a little quick for No.2 as compared with No.3.

The inclined crack in the joint initiated near the corner of the joint most quickly at P = 2t for No.2. Thereafter the inclined cracks occurred near the center of the joint, but the crack width was not so large and about 0.1mm. For No.1 the propagation of the inclined crack was about the same as for No.2 except that it was a little slow and the crack width was relatively large and about 0.2mm. The inclined crack initiated most slowly at P = 4t for No.3 and thereafter propagated from the center to the compression corner. Analytical results on the initial inclined cracking load gave good agreements with test results.

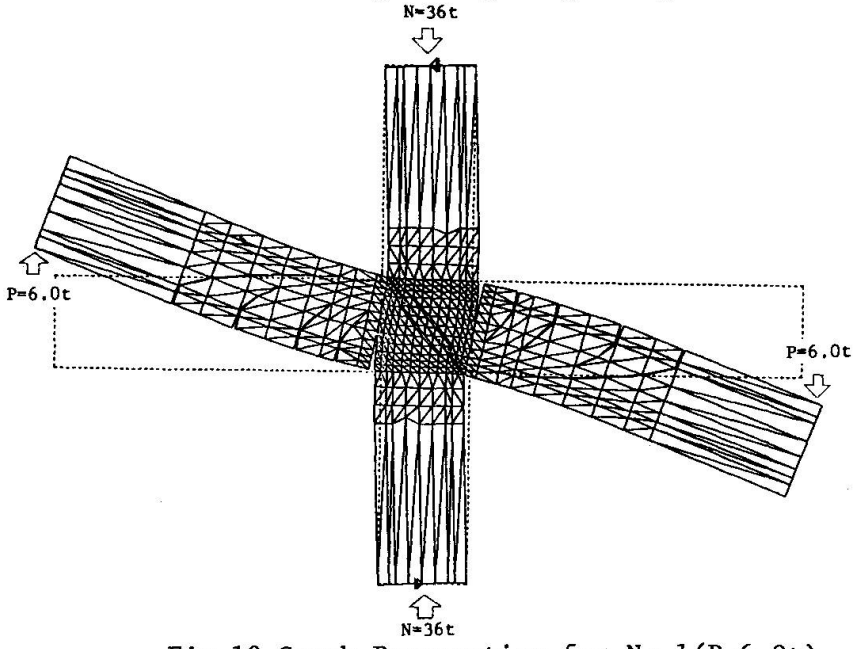

Fig.10 Crack Propagation for No.1(P=6.0t)

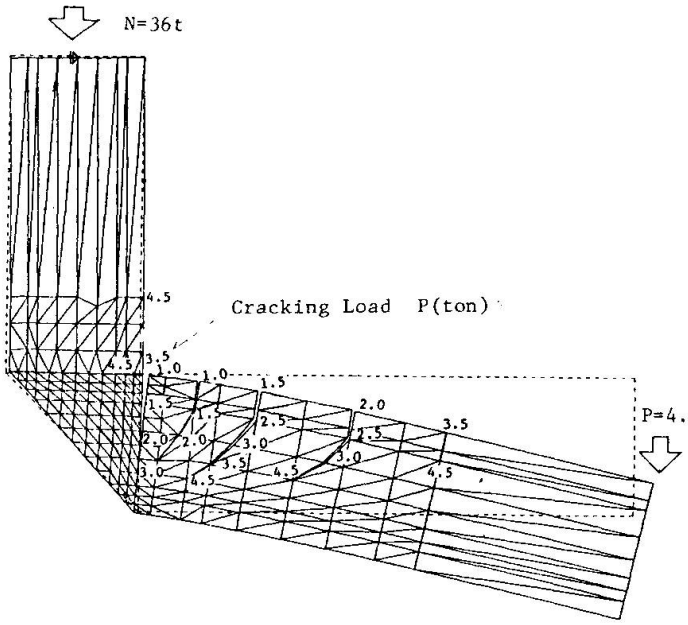

Fig.9 Crack Propagation for No.1(P=4.5t)

Table 2. Comparisons of Analytical Results with Test Results

	Calculated	No.1	No.2	No.3	No.4
Beam Flexural Crack	1.0	1.0 (1.3)	1.0 (1.0)	1.0 (1.0)	1.0
Column Flexural Crack	3.3	3.5 (3.0)	4.0 (2.5)	4.0 (3.0)	4.0
Joint Inclined Crack	2.8	3.0 (3.0)	2.0 (2.5)	4.0 (4.0)	-
Beam Shear Crack	3.3	3.0 (3.5)	3.5 (3.5)	3.0 (3.5)	3.0
Beam Bar Yielding	7.9	9.5 (6.5)	9.6 (6.0)	- (-)	-
Yielding in P-δ Curve of Test		(7.3)	(6.3)	(6.0)*	

Note: ( ):Test Result. Unit(ton)
Calculated: obtained by the theoretical or experimental equation.
* :Compression Failure of Concrete

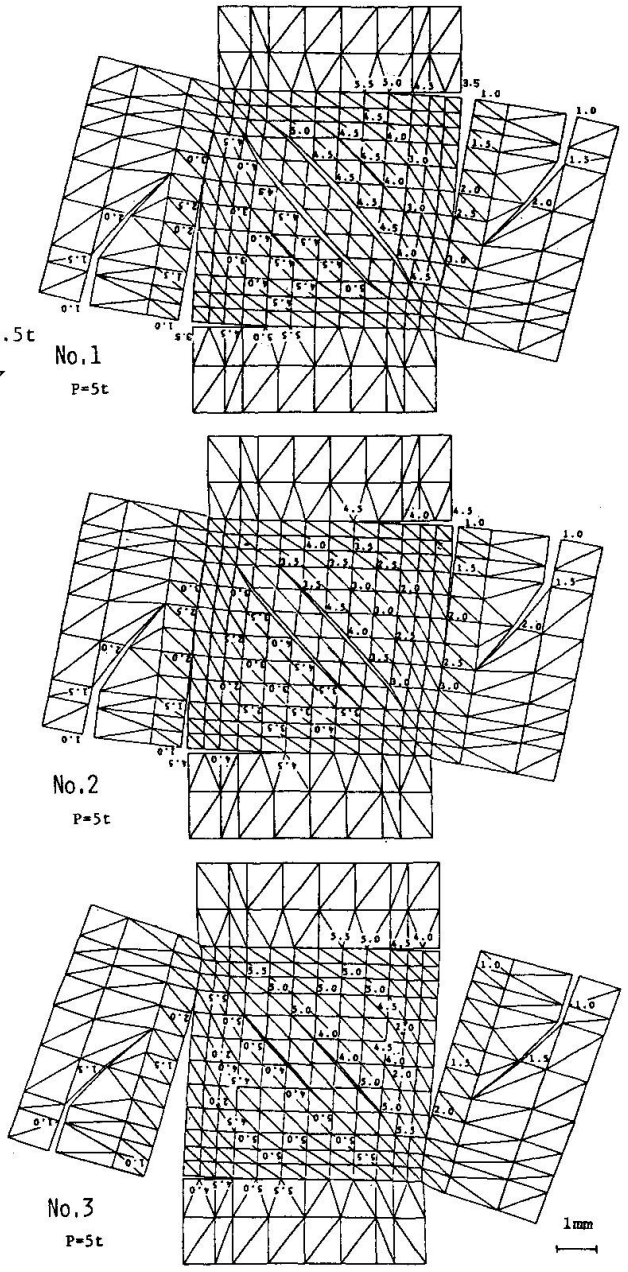

Fig.11 Deformation of Joints and Their Vicinities

The flexural yielding of the beam occurred at P = 9.5t, 9.6t respectively for No. 1, No.2. The analytical result, P = 9.5t is rather higher than the test results, P = 7.3t for No.1. For No.3 the flexural yielding did not occur. This is corresponding to the test result.

The local compressive failure of concrete occurred at the beam joint at P = 6 - 7t and thereafter began to occur in the center of the joint for No.1 and No.3.

6. LOAD-DEFLECTION RELATIONSHIPS

The load-deflection curves for the test and the analytical model are shown in Figs. 12 through 15. The analytical results were obtained in accordance with

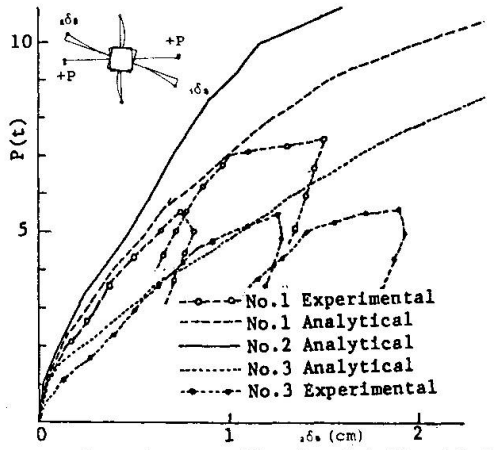

Fig.12 Load-Beam Deflection Relationships

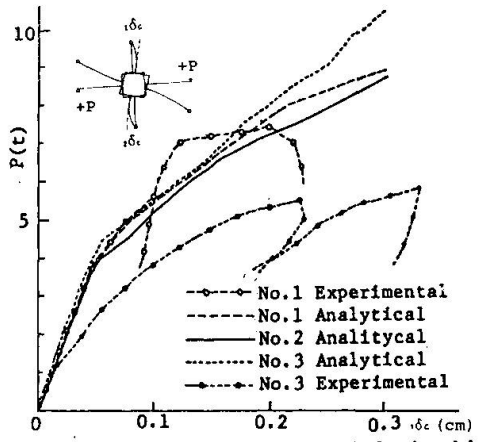

Fig.13 Load-Column Deflection Relationships

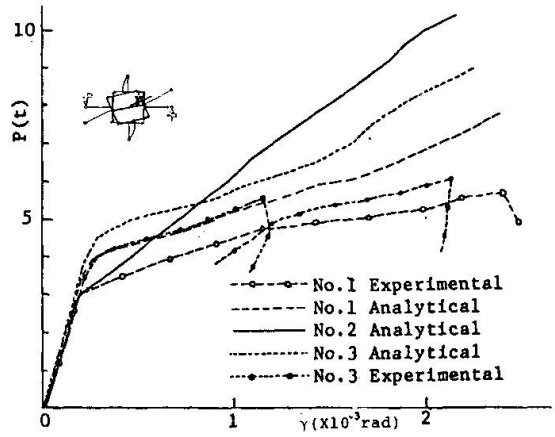

Fig.14 Load-Joint Distortion Relationships

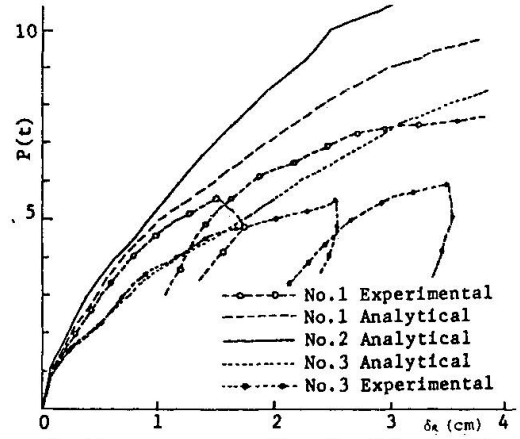

Fig.15 Load-Story Deflection Relationships

the measuring method in the tests as well as possible.

For No.1 the analytical model predicted a higher yield strength than was actually obtained, but gave a good match with the load-deflection behavior to the yield strength obtained in the test except that the analytical joint distortion proved to be a little stiff.

For No.3 the analytical model also obtained a good agreement with test results to P = 5.5t except that the analytical column deflection proved to be stiff.

The beam deflection increased as the bond chracteristics became poorer. These phenomena are considered to be based on the effect of bond slip of beam bars through the joint.

The column deflections were almost the same for all specimens to P = 4t, but thereafter No.3 proved to be slightly stiff and an opposite tendency was developed as compared with the beam deflection.

The initial stiffness of the joint distortion was almost the same for all specimens, but No.2 proved to be rather stiff even after the initiation of the inclined crack as compared with No.1 and No.3.

The story deflection of each specimen was subjected to the great influence of the beam deflection.

7. STRAIN AND BOND SLIP OF BEAM LONGITUDINAL BARS

The strain distributions of beam longitudinal bars for the test and the analytical model are shown in Fig. 16.

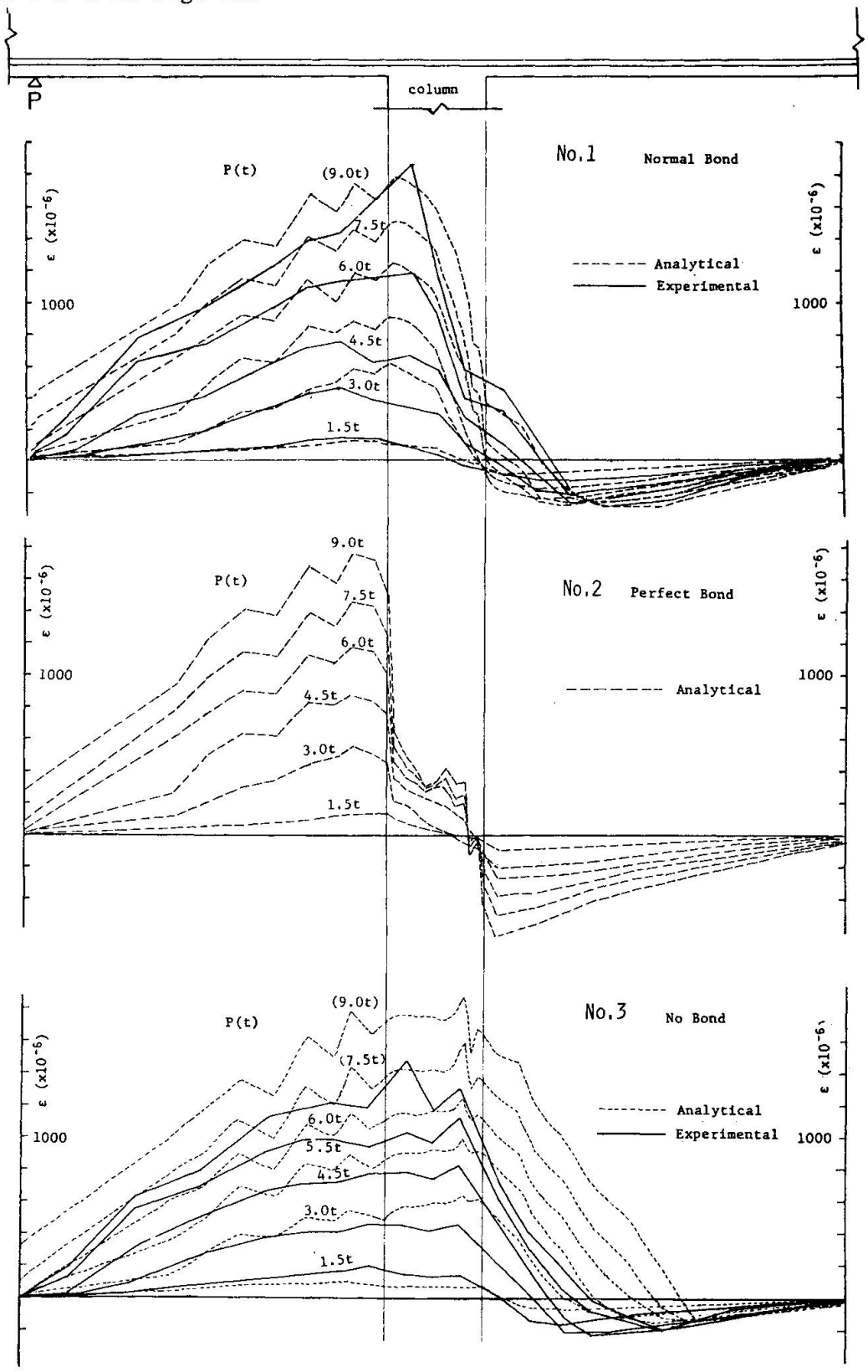

Fig.16 Strain Distributions of Beam Bottom Bars

The bond slips of beam longitudinal bars through the joint for the test and the analytical model are shown in Fig. 17.

The analytical results obtained a good agreement with test results for No.1, except the transformation of the compressive strain of beam longitudinal bars to tensile strain appeared a little later near the joint than test results and the sinking of beam bar into the joint proved to be a little smaller than test results.

From the analytical results for No.2 with almost perfect bond, it can be stated that the tensile strain of beam bars decreases greatly inside the joint and the transformation of the compressive strain of beam bars to tensile strain did not appear very conspicuously even inside the joint. This phenomenon indicated that the truss mechanism after the initiation of the inclined crack had not so great influence on the strain distribution of beam bars through the joint with the tie ratio, p_w = 0.7 %.

Meanwhile analytical results for No.3 obtained a good agreement with test results and show that the bond slips of beam bars through the joint increased remarkably and the tensile stress of beam bars at the beam joint was transferred directly to the compression zone through the joint. As the result the transformation of the compressive strain of beam bars to tensile strain was very noticeable.

As there was no great difference between the analytical results for No.3 and No.4, the effect of the loss of bond on the strain distribution of beam bars through the joint appeared to be much greater than that of the truss mechanism which was developed by the inclined crack.

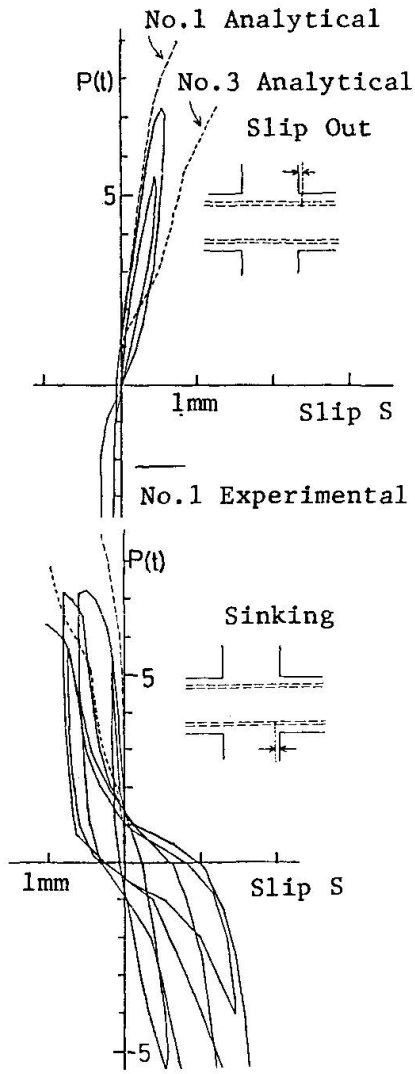

Fig.17 Bond Slip of Beam Bars through Joints

8. STRAIN OF COLUMN LONGITUDINAL BARS

The analytical results of strain distribution of column longitudinal bars showed almost the same tendencies for No.1, No.2 and No.3.

Fig. 18 shows the strain distribution of column bars for No.1. The transformation of the compressive strain to tesile strain appeared at about P = 6t, and this phenomenon is corresponding to the test result.

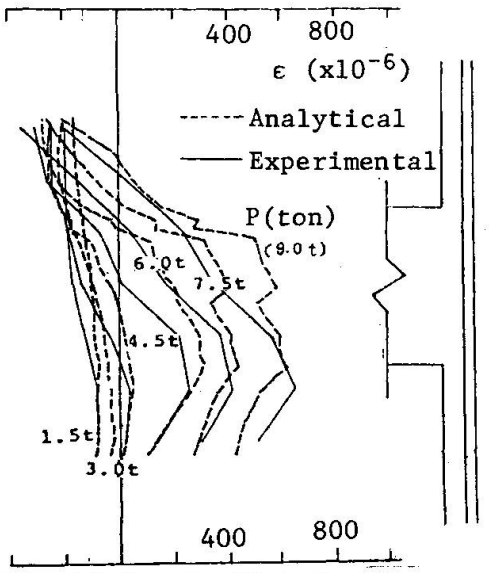

Fig.18 Strain Distributions of Column Longitudinal Bars

9. STRAIN OF TIES

Fig. 19 shows the strain of ties inside the joint for the test and the analytical models. The analytical strain of ties began to increase after the inclined crack initiated.

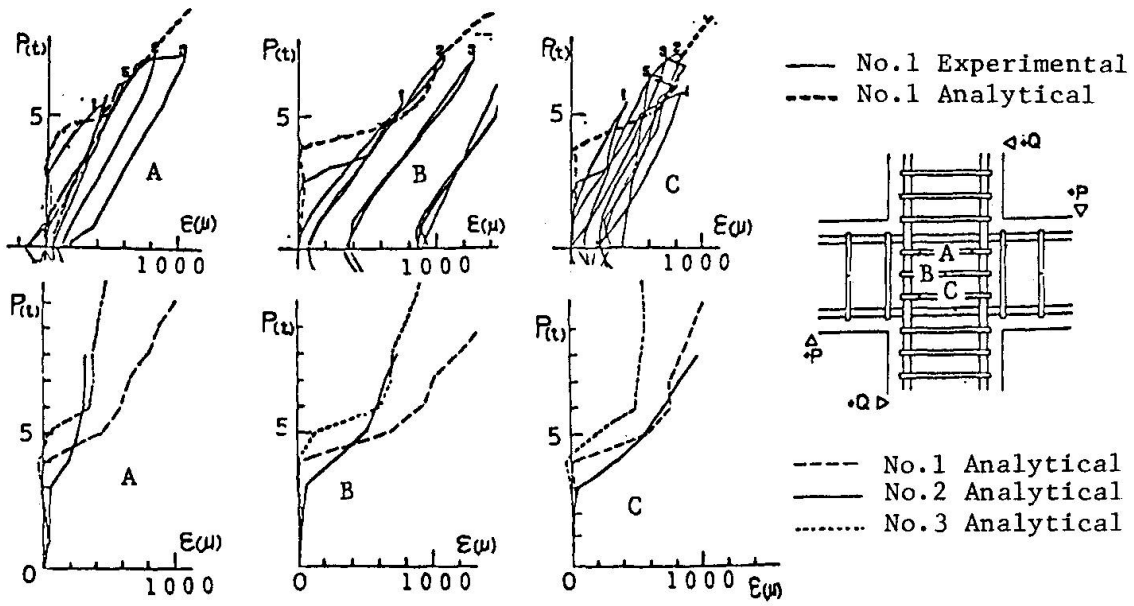

Fig.19 Relationships between Load and Strain of Ties

These phenomena were also observed a little later in the test results.

The strain of ties for No.3 appeared to be relatively smaller than that for No.1, but the effect of bond characteristics of beam bars on the strain of ties was not so remarkable.

10. TRUSS MECHANISM AND LOSS OF BOND

Fig. 20 shows the analytical stress distribution in the joint for No.2 and No.4. For No.2 with almost perfect bond for beam bars only the effect of the truss mechanism was designed to appear after the inclined crack initiated. For No.4, in which the initiation of inclined cracks were prohibited and almost no bond was assumed for beam bars, only the effect of the loss of bond was designed to appear.

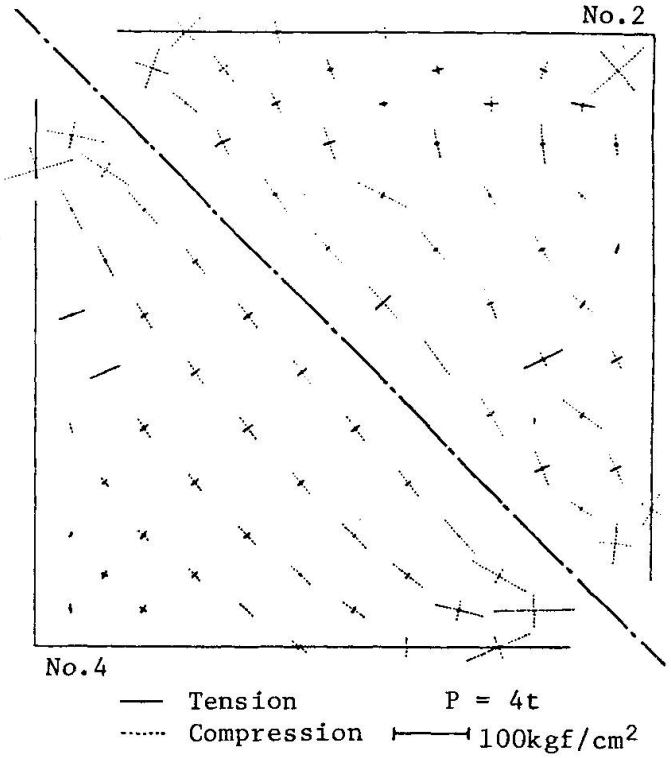

Fig.20 Stress Distributions of Joints

In No.2 the truss mechanism was observed and the higher compressive stresses were concentrated upon the center strut of the joint. But the stresses were dispersed by the bond near the end of the joint and the concentration of stresses upon the compression corner was not so marked.

In No.4 the flow of stress had a wide range in the center of the joint, but the compressive stress concentration was conspicuous at the compression corner from the loss of bond. The local compression failure of concrete at the beam joint was considered to be caused primarily by this phenomenon.

11. CONCLUSIONS

The nonlinear behaviors of reinforced concrete beam-column joints, such as the transformation of strain distribution of beam bars or the bond slip of beam bars through the joint, were analyzed by the finite element model combining the individual material properties.

From the comparison of analytical results for the normal bond (No.1) and almost no bond (no.3) for beam bars through the joint, it could be stated that analytical model predicted a higher yield strength of the beam for No.1, but the analytical load-deflection behavior after the initiation of the inclined crack, various cracking load and the strain distribution of beam bars gave a good match with test results.

The principal cause of higher yield strength of the beam obtained in the analysis was to be sought in not considering the downward sloping portion of the stress-strain curve of concrete after the compressive strength in the analytical model. Really in the test the transformation of the compressive strain of beam bars to tensile strain and the compressive stress concentration near the beam joint from the bond deterioration caused the local compression failure of concrete. It will be necessary to add the modeling of the downward sloping portion of the stress-strain curve to this model.

From the comparison of the truss mechanism model, No.2, with the loss of bond model, No.4, it could be stated that the transformation of strain distribution of beam bars, which had a great influence on the shear resistance mechanism of the joint, was more seriously affected by the loss of bond than by the truss mechanism.

It was recognized from this study that the bond slip through the joint from the bond deterioration not only increased the story deflection, but also changed the stress distribution of concrete and beam bars in the joint and brought about the transformation of compressive strain of beam bars to tensile strain and the local compression failure of concrete. These phenomena will be a primary factor to decrease the flexural yield strength of beams and deteriorate the restoring force characteristics of the overall structures.

It was known that the bond deterioration was severer in the case of cyclic loading [24], [25], [26], [33]. In the further work it will be necessary to study the effect of bond deterioration under load cycles on the behavior of the beam-column joint.

ACKNOWLEDGEMENTS

This study was supported by the Kohzoh Keikaku Engineering. The autor wishes to express his sincere gratitude to Professor Emiritus H. Umemura and Professor H. Aoyama at the University of Tokyo for their warmhearted guidance and encouragement.

REFERENCES

1. Jirsa, J.O., Aleman, M.A. and Meinheit, D.F., "Influence of Lateral Beams on the Behavior of Beam-Column Joints," 6th World Conf. on Earthquake Engrg., New Delhi, Jan. 1977.
2. Umemura, H., Hamada, D., Kamimura, T. and Takada, M., "Experimental Study on Reinforced Concrete Beam-Column Joints with Eccentric Wallgarder Beams," Proc. Annual Conv., Architectural Institute of Japan (AIJ), Sep. 1980, pp.1517-1520.
3. Burguiers, S.T., Jirsa, J.O. and Longwell, J.E., "The Behavior of Beam-Column Joints under Bidirectional Load Reversals," Bulletin D'information, No.132, AICAP - CEB Symposium, Rome, May 1979, pp.221-228.
4. Shimohira, F. and Higashi, Y., "Analysis of Reinforced Concrete Beam-Column Joint by Finite Element Method," Proc. Annual Conv., AIJ, Nov. 1971, pp.843-844.
5. Will, G.T., Uzumeri, S.M. and Sinha, S.K., "Application of the Finite Element Method to the Analysis of Reinforced Concrete Beam-Column Joints," Proc. of the Speciality Conf. on FEM in Civil Engrg., CSCE, EIC, Canada, Jun. 1972, pp.745-766.
6. Mirza, M.S. and Mufti, A.A., "Nonlinear Finite Element Analysis of Reinforced Concrete Structures," Proc. of the 1974 International Conf. on FEM in Engrg., Univ. of New South Wales, Australia, 1974, pp.403-417.
7. Ohtsuki, K. and Obata, M., "Elasic Plastic Analysis of Infinitely Uniform Frames by Finite Element Method," Proc. Annual Cov., AIJ, Oct. 1975, pp.771-772.
8. Ohwada, Y., "Stress Analysis of Reinforced Concrete Beam-Column Joint Subjected to Seismic Stress: Three-Dimensional Elastic Analysis by FEM," Proc. Kanto Dist. Symp., AIJ, Jul. 1979, pp.185-188.
9. Ichinose, T. and Aoyama, H., et al., "Nonlinear Analysis of Reinforced Concrete Rectangular Frame Considering the Continuity of Reinforcement," Proc. Kanto Dist. Symp., AIJ, Jul. 1980, pp.137-140.
10. Tada, T. and Takeda, T., "Analytical Study on Deformation Characteristics of Plastic Hinge at the End of RC Memeber and Process of Bond Deterioration in Neighbouring Anchorage Zone," Proc. Kanto Dist. Symp., AIJ, Jul. 1980, pp.125-132.
11. Felippa, C.A., "Refined Finite Element Analysis of Linear and Nonlinear Two-Dimensional Structures," SESM Report, No.66-22, Univ. of California, Berkeley, Oct. 1966.
12. Darwin, D. and Pecknold, D.A., "Nonlinear Biaxial Stress-Strain Law for Concrete," Jour. Engr. Mech. Div., ASCE, vol.103, No.EM2, Apr. 1977, pp.229-241.
13. Darwin, D. and Pecknold, D.A., "Analysis of R.C. Shear Panels Under Cyclic Loading," Jour. Struct. Div., ASCE, Vol.102, No.ST2, Feb. 1976, pp.355-369.
14. Darwin, D. and Pecknold, D.A., "Inelastic Model for Cyclic Biaxial Loading of Reinforced Concrete," SRS No.409, Univ. of Illinois at Urbana-Champaign, Jul. 1974.
15. Noguchi, H., "Finite Element Nonlinear Analysis of Reinforced Concrete: Part 1: Stress-Strain Relationships of Concrete under Biaxial Stresses," Trans. of AIJ, No.252, Feb. 1977, pp.1-11.
16. Aoyama, H. and Noguchi, H., "Mechanical Properties of Concrete under Load Cycles Idealizing Seismic Actions," Bulletin D'information, No.131, AICAP - CEB Symposium, Rome, May 1979, pp.31-63.
17. Kupfer, H.B. and Grstle, K.H., "Behavior of Concrete under Biaxial Stresses," Jour. Engr. Mech. Div., ASCE, Vol.99, No.EM4, Aug. 1973, pp.853-866.
18. Nelissen, L.J.M., "Biaxial Testing of Normal Concrete," Heron, Delft, Vol.18, No.1, 1972.
19. Saenz, L.P., Disc. of "Equation for the Stress-Strain Curve of Concrete," by Desayi and Krishnan, ACI J., Proc. Vol.61, No.9, Sep. 1964, pp.1229-1235.

20. Kupfer, H.B., Hilsdorf, H.K. and Rüsch, H., "Behavior of Concrete under Biaxial Stresses," ACI J., Proc. Vol.66, No.8, Aug. 1969, pp.656-666.
21. Ngo, D. and Scordelis, A.C., "Finite Element Analysis of Reinforced Concrete Beams," ACI J., Proc. Vol.64, No.3, Mar. 1967, pp.152-163.
22. Noguchi, H., "Finite Element Nonlinear Analysis of Reinforced Concrete: Part 2: Mechanics of Bond and Slip of Deformed Bars in Concrete," Trans. of AIJ, No.258, Aug. 1977, pp.27-37.
23. AIJ Structural Standard Committee and R.C. Structural Subcommittee, "Bond Characteristics: Part 2," Series 12, Materials for Ultimate Strength Design of R.C., Jour. of Arch. and Building Science, AIJ, Vol.95, Jan. 1980, pp.61-62.
24. Morita, S. and Kaku, T., "Local Bond Stress-Slip Relationship under Repeated Loading," Proc. IABSE Symp., Lisbon, Portugal, Sep. 1973.
25. Morita, S. and Kaku, T., "Bond-Slip Relationship under Repeated Loading," Trans. of AIJ, No.229, Mar. 1975, pp.15-24.
26. Tassios, T.P., "Properties of Bond between Concrete and Steel under Load Cycles Idealizing Seismic Actions," Bulletin D'information, No.131, AICAP - CEB Symposium, Rome, May 1979, pp.65-122.
27. Noguchi, H., "Finite Element Nonlinear Analysis of Reinforced Concrete: Part 4: Crack Initiation and Propagation," Trans. of AIJ, No.262, Dec. 1977, pp.43-52.
28. Zienkiewicz, O.C., "The Finite Element Method in Engineering Science," Second Edition, McGraw-Hill, 1971.
29. Zienkiewicz, O.C., "The Finite Element Method," Third Edition, McGraw-Hill, 1977.
30. Yamada, Y., "Plasticity and Visco-elasticity," Baifuhkan, 1972.
31. Kamimura, T. and Hamada, D., et al., "Experimental Study on Reinforced Concrete Beam-Column Joints: Part 1 - 3," Proc. Annual Conv., AIJ, Sep. 1978, pp.1673-1674, Sep. 1979, pp.1303-1306.
32. Tada, T., Takeda,T. and Takemoto, Y., "Tests on Bond Characteristics of Deformed Bars: Process of Bond Deterioration in the Beam-Column Joints," Proc. Kanto Dist. Symp., Jul. 1977, pp.229-232.
33. Gerstle, K.H., "Material Modeling of Reinforced Concrete," Inductory Report of IABSE Colloquium, Delft 1981, IABSE - AIPC - IVBH, Oct. 1980, pp.41-61.